PFC/JA-82-3

THE FAR UV EMISSION SPECTRUM OF H_2

J. L. Terry

Plasma Fusion Center
Massachusetts Institute of Technology
Cambridge, MA 02139

September 1982

This work was supported by the U.S. Department of Energy Contract No. DE-AC02-78ET51013. Reproduction, translation, publication, use and disposal, in whole or in part by or for the United States government is permitted.

THE FAR UV EMISSION SPECTRUM OF H_2

J. L. Terry

Plasma Fusion Center

Massachusetts Institute of Technology

ABSTRACT

A detailed, quantitative model is constructed to describe excitation of the B $^1\Sigma_u^+$ and a $^3\Sigma_g^+$ states in molecular hydrogen by thermal electrons with 1 eV < T_e < 10 eV and densities < 10^{15} cm^{-3}. The resulting radiative decay is also quantitatively modeled, and synthetic Far UV spectra are produced. These synthetic spectra are compared with measured laboratory spectra from three sources, one of which is the high temperature discharge of the Alcator C tokamak. The agreement is quite good.

A cross-section of $1 \times 10^{-18} (E_{th}/E)^2$ cm^2 is deduced for electron excitation from X $^1\Sigma_g^+$ to a $^3\Sigma_g^+$.

I. Introduction

It is an obvious but often neglected fact that molecular hydrogen is a constituent of the edge plasma in present day, high temperature, magnetically confined plasmas. Molecular hydrogen has been studied by Hinnov et al.[1] in C Stellarator discharges; it was noted by McNeill[2] as the source of background light complicating Thompson scattering measurements, and was observed by the author[3] in Alcator C plasmas.

Quantitative knowledge of the edge plasma in fusion-grade plasmas is important in attempting solution of the following major problems:

1) it is not yet understood how gas molecules, injected at the plasma edge, are ingested by the plasma;
2) it is not quantitatively understood how the density profile is maintained;
3) particle 'recycling', the loss of plasma particles to material walls and limiters and the return of neutral particles (atoms or molecules?) to the plasma edge is not quantitatively understood.

Molecular hydrogen may play a role in each of these processes. In quantifying that role, knowledge of the molecular density, temperature, ionization rate, dissociation rate, and the energy distribution of the dissociation products is quite useful.

It is the purpose of this paper to review and extend the models which allow determination of some of the quantities relating to the transport, ionization and dissociation of H_2 from knowledge of the shape and intensity of its plasma-produced, Far UV spectrum. It is an extension of similar

work by Ajello, et al.[4], in which they synthesized Werner and Lyman band emission, resulting from monoenergetic electron excitation, and applied the formalism to spectra from the Jovian Aurora[5].

Molecular hydrogen is most easily observed spectroscopically, specifically in the Far UV region of the spectrum from ~ 1300 Å to ~ 2200 Å. A Far UV spectrum of H_2 emitted from a $T_e \sim 1$ eV, $n_e \sim 10^{13}$ cm^{-3} plasma is shown in Figure 1.

The major features of the spectrum shown in Fig. 1 are a result of transitions which involve the four electronic states with potential energy curves[6] shown in Fig. 2. They are the two lowest electronic states in the singlet system (the ground state, X $^1\Sigma_g^+$, and the B $^1\Sigma_u^+$ state), and two lowest in the triplet system, one of which (b $^3\Sigma_u^+$) is repulsive. The observed emissions result from: 1) excitation from rotational-vibrational levels of the ground state to the rotational-vibrational levels of the B $^1\Sigma_u^+$ state with subsequent radiative decay to bound ground state levels (the Lyman bands) and to a continuum of vibrational levels above the dissociation limit in the ground state (the Lyman continuum); and 2) optically-forbidden electron impact excitation from the ground state levels to the a $^3\Sigma_g^+$ levels, followed by the allowed radiative decay to the repulsive b $^3\Sigma_u^+$ state (the H_2 continuum).

The quantitative models for these processes are presented as follows: The distribution among the ground state levels is described in Section III. The excitation to and decay from the B $^1\Sigma_u^+$ levels are described in Sections IV and V. The 'forbidden' excitation to the a $^3\Sigma_g^+$ levels and the subsequent dissociation by decay to the b $^3\Sigma_u^+$ state are discussed in Section VI. The extent to which the synthetic spectra, constructed on the

basis of these models, are able to reproduce the measured spectra is examined in Section VII.

II. The Measured Spectra

In justifying the applicability of these models, experimental spectra from three sources, measured by two monochromators, are presented. The spectrum shown in Fig. 1 is emitted by the low temperature plasma created in the Alcator C tokamak[7] for the purpose of wall conditioning before a day's series of high temperature discharges. This is called 'discharge cleaning' (also Taylor Discharge Cleaning[8]). The electron temperature is probably between 1 and 3 eV, since the doppler broadening of Hα indicates that the ion temperature is 1 eV. The electron (and ion) density is in the range from 3×10^{12} to 3×10^{13} cm^{-3}, based on measurements of the filling pressure (5×10^{-4} torr of H_2) and assuming 10-100% ionization.

The spectrum shown in Fig. 6 was emitted during a tokamak discharge, when the central electron and ion temperatures are ~ 1000 eV, and central plasma densities are $\sim 5 \times 10^{14}$ cm^{-3}. Of course, the molecular hydrogen exists only at the periphery of this discharge, where the electron temperature is 1-10 eV, and the electron density is from 1×10^{13} to a few $\times$ 10^{14} cm^{-3}.

Both of the these spectra were measured by a 1/8th m, absolutely calibrated, vacuum monochromator with a resolution of 3 Å and a spectral range from 1200 to 2300 Å. In each of the spectra the response of the instrument has been compensated.

The third spectrum, shown in Fig. 3, was produced by an H_2 discharge lamp of the type described by Fastie and Kerr[9]. The H_2 pressure in the lamp is ~ 0.4 Torr, and the H_2 kinetic temperature is ~ 470 °K. The high resolution spectrum was measured by G. H. Mount with a 0.5 m vacuum monochromator. The instrumental resolution was ~ 0.15 Å.

III. The Ground State $X\ ^1\Sigma_g^+$

It is assumed here that the great majority of the molecules are in the ground electronic state. In addition, it is assumed that the distribution among the rotational-vibrational levels of the ground state only is close to a thermal one; i.e. it can be represented by a Maxwell-Boltzmann factor times the level degeneracy

$$n_{v",j"} = \frac{N_0}{U}\, g(I)\, g(j")\, e^{-E_{v"j"}/T} \qquad \text{(Eq. 1)}$$

where the double-primed quantities label the ground state vibrational-rotational levels from which the excitation occurs,

N_0 is the molecular density (in cm^{-3}, for example),

$g(I) = 2I + 1$ is the degeneracy due to the total nuclear spin,

$g(j") = 2j" + 1$ is the rotational degeneracy,

$E_{v"j"}$ is the energy of the v",j" level above the v" = 0, j" = 0 level[10, 11],

$U = \sum_{v",j"} n_{v"j"}/N_0$ is the partition function,

and T is the 'H_2 temperature', describing the thermal distribution.

Ultimately this distribution must be established and maintained by collisions, either with electrons of temperature T_e, with ions, with other H_2 molecules, or with the H atoms which are also present. The cross-sections, excitation rate coefficients, and transition probabilities for most of these processes are found in [12, 13, 14, 15, 16, 17]. The cross-section for excitation (and deexcitation) by electrons is by far the largest, and therefore in a plasma the 'H_2 temperature' should approach the local electron temperature. However, it is beyond the scope of this paper to examine this collisional process, so the electron temperature and the 'H_2 temperature' will be treated as independent throughout.

The presence of nuclear spin and the fact that the nuclei which make up H_2 are identical fermions have interesting and observable consequences. It is a fundamental property that the total wavefunction of a state made up of identical fermions must be antisymmetric upon exchange of any two. In the case of H_2, the total wavefunction may be represented as a product of a nuclear spin part $|I\rangle$ and a part which depends upon the actual particle coordinates $|\Psi\rangle$. The properties of these parts upon exchange of the nuclei are[11]:

$|I\rangle \rightarrow |I\rangle$ for ortho-hydrogen, where I = 1 (nuclear spins 'parallel')

$|I\rangle \rightarrow -|I\rangle$ for para-hydrogen, where I = 0 (nuclear spins 'anti-parallel')

$|\Psi\rangle \rightarrow |\Psi\rangle$ for a Σ_g^+ state with even j"

$|\Psi\rangle \rightarrow -|\Psi\rangle$ for a Σ_g^+ state with odd j"

$|\Psi\rangle \rightarrow -|\Psi\rangle$ for a Σ_u^+ state with even j"

and $|\Psi\rangle \rightarrow |\Psi\rangle$ for a Σ_u^+ state with odd j".

Thus ortho-hydrogen (with a nuclear spin degeneracy of 3) has a ground state with only odd j"s and a B $^1\Sigma_u^+$ state with only even j"s. Para-hydrogen (with nuclear spin degeneracy of 1), on the other hand, has a ground state with only even j"s and a B $^1\Sigma_u^+$ state with only odd j"s. The ground state density is

$$n_{v"j"} = \frac{N_o}{U} \begin{Bmatrix} 3 - j" \text{ odd} \\ 1 - j" \text{ even} \end{Bmatrix} (2j" + 1)\, e^{-E_{v"j"}/T}$$

The conservation of angular momentum for dipole transitions between Σ states allows only changes of ± 1 in the rotational quantum number j. This allows dipole transitions between the existing rotational levels of X $^1\Sigma_g^+$ and B $^1\Sigma_u^+$ in both ortho- and para-hydrogen. Thus when observing a source with a mixture of both, one finds an intensity alternation in the lines originating from a sequence of rotational levels. The magnitude of the intensity alternation is influenced by the nuclear spin through its degeneracy. Furthermore, the oddness or evenness of the rotational level from which the more intense emission arises is a direct consequence of the particle statistics of the nuclei.

IV. Densities of the B $^1\Sigma_u^+$ State.

The densities in the B $^1\Sigma_u^+$ state are determined by a balance between collisional excitation from the X $^1\Sigma_g^+$ state and radiative decay to that state.

$$\sum_{v,j} A_{vj}^{v'j'}\, n_{v'j'} = \sum_{v",j"} Q_{v"j"}^{v'j'}(T_e)\, n_e\, n_{v"j"} \qquad \text{(Eq. 2)}$$

where the primed quantities label the upper state levels,

the double primed quantities label the ground state levels from which excitation occurs,

the unprimed quantities label the lower state levels to which the system decays,

$A_{v'j'}^{v''j''}$ is the transition probability (sec^{-1}),

$Q_{v''j''}^{v'j'}(T_e)$ is the excitation rate coefficient (cm^3/sec),

n_e is the local electron density (cm^{-3}),

and $n_{v''j''}$ is the ground state density (cm^{-3}), given by Eq. 1.

(Eq. 2 implies that contribution by cascade to $n_{v'j'}$ is negligible. Ajello, et al.[4] maintain that cascade from the E,F $^1\Sigma_g^+$ levels may be important, especially in leading to emission around 1350Å.)

A. The Excitation Rate Coefficients, $Q_{v''j''}^{v'j'}(T_e)$

It is assumed that the peak in the cross-section for excitation between vibrational levels is proportional to the matrix element for a dipole transition, i.e. $f_{v''}^{v'}/E_{v''}^{v'}$ where f is the oscillator strength, and E is the energy difference between the levels. The constant of proportionality is calculated from the total cross-section for excitation from v" = 0, measured by Ajello, et al.[4], and the shape of the cross-section is taken from Fig. 5 of the same reference. After multiplication by the electron velocity and integration over a Maxwellian, it is found that the excitation rate coefficient for excitation to vibrational levels of the B $^1\Sigma_u^+$ state is well fit (for $1 < T_e < 10$ eV) by

$$Q_{v''}^{v'}(T_e)(cm^3/sec) = \frac{4.26 \times 10^{-4}\ f_{v''}^{v'}}{E_{v''}^{v'}}\ e^{-g(E_{v''}^{v'})/T_e} \qquad \text{(Eq. 3)}$$

where $f_{v''}^{v'}$ is the oscillator strength[18],

$E_{v''}^{v'}$ is in cm^{-1},

$g(E_{v''}^{v'}) = 1.18 \times 10^{-3} (E_{v''}^{v'})^{0.80971}$,

and T_e is the electron temperature in eV.

The energies of the B $^1\Sigma_u^+$ levels were taken from [10,11]. The excitation of specific rotational levels within a vibrational level is accounted for by multiplying by the rotational line strength and dividing by the rotational degeneracy of the initial state $(2j'' + 1)$[11]; i.e.,

$B_e^R(j') = j'/(2j' + 3)$ for R branch excitations (i.e., $j_{upper} - j_{lower} = 1$),

$B_e^P(j') = (j' + 1)/(2j' - 1)$ for P branch excitations (i.e., $j_{upper} - j_{lower} = -1$).

Thus $Q_{v''j''}^{v'j'} = B_e(j')Q_{v''}^{v'}$ with $Q_{v''}^{v'}$ given by Eq. 3.

B. The Transition Probabilities from the B $^1\Sigma_u^+$ State

The quantity $\sum_{v,j} A_{vj}^{v'j'}$ is the inverse of the (radiative) lifetime of the v',j' state. The lifetimes of the v' levels of the B $^1\Sigma_u^+$ state are given by Stephens and Dalgarno[19]. The rotational levels are dealt with in an analogous manner, multiplying by the line strength and dividing by the rotational degeneracy of the initial state of the transition $(2j' + 1)$;

$B_d^R(j') = j'/(2j' + 1)$ for R branch decays,

$B_d^P(j') = (j' + 1)/(2j' + 1)$ for P branch decays.

Note that the sum over rotational decay channels from a specific j' level

is 1, so that $\sum_{v,j} A_{vj}^{v'j'} = \sum_{v} A_{v}^{v'}$.

V. Lyman Emission

A. Bound-bound Transitions

Once the upper level populations, $n_{v'j'}$, are determined (by Eqs. 1, 2, and 3), the volume emission rate of photons arising from a transition from the v',j' level of the B $^1\Sigma_u^+$ state to the v,j level of the ground state is

$$I_{vj}^{v'j'}(\text{photons/cm}^3\text{sec}) = A_{vj}^{v'j'}\, n_{v'j'} = B_d\, A_v^{v'}\, n_{v'j'}, \qquad \text{(Eq. 4)}$$

where $A_v^{v'}$ is the transition probability, found in [18].

Fig. 3 shows the good agreement between the spectrum predicted by this model and a high resolution, measured spectrum.

B. The Lyman Continuum

This continuum emission was first identified by Dalgarno, Herzberg, and Stephens[20] in 1970. Although the emission exists from ~ 1150 Å to ~ 1650 Å, it peaks in a 50 Å region around 1575 Å. This peak results from a maximum in the overlap integral between vibrational continuum wavefunctions of the ground state, with energies just greater than the dissociation energy, and the $v' \approx 9$ wavefunctions of the B $^1\Sigma_u^+$ state. This is shown schematically in Fig. 4. Note the vertical overlap between the wavefunctions at $R \sim 4.5$ atomic units. For continuum emission one calculates a volume emission rate $I^{v'j'}(\lambda)d\lambda$ for photon emission within

the bandpass λ to $\lambda+d\lambda$. In addition, one requires the density of continuum states in the calculation of the transition probability for a transition resulting in a photon within that bandpass. From [21, 19, 22]

$$I^{v'j'}(\lambda)d\lambda = \frac{128(\pi^4)c}{3} \rho^{v'}(\lambda)|\langle f|\vec{e}\cdot\vec{p}|B_{v'j'}\rangle|^2 n_{v'j'}d\lambda/\lambda^5 \qquad \text{(Eq. 5)}$$

where $\rho^{v'}(\lambda)$ is the density of continuum states an energy hc/λ below the v',j' level of the $B\ ^1\Sigma_u^+$ state,

and $\langle f|\vec{e}\cdot\vec{p}|B_{v'j'}\rangle$ is the dipole matrix element connecting the initial bound state $|B_{v'j'}\rangle$ with the final state $|f\rangle$, one of a large number of continuum states with an energy hc/λ below the initial state.

The vibrational continuum wavefunctions are normalized within a sphere of radius L, so that for very large nuclear separation R they approach

$$|f\rangle \sim \left(\frac{2}{L}\right)^{1/2} \sin(kR + \phi),$$

and the density of continuum states becomes

$$\rho^{v'}(\lambda) = \frac{L}{h} \left(\frac{m_p}{E_k}\right)^{1/2}$$

where m_p is the proton mass,

and E_k is the energy of the final vibrational state above the dissociation limit.

The dipole matrix elements connecting each vibrational level of the $B\ ^1\Sigma_u^+$

state to continuum states an energy hc/λ below it have been calculated by Stephens[22] for 1150 Å < λ < 1650 Å in 1Å intervals. These matrix elements and a computer program calculating the Lyman continuum for any specified upper state distribution were kindly supplied to the author by A. Dalgarno.

For this emission the rotational structure has not been taken into account, i.e. only transitions between vibrational levels were considered. However, it is expected that the major effect of rotation is simply a washing out and broadening of the finer spectral structure. This may be understood qualitatively as follows: If one imagines adding rotational energy, $E_{rot} \propto j(j+1)/R^2$, to potential curves of similar shape, the resulting radial shift in each vibrational wavefunction will be approximately the same. Thus, the overlap integral between vibrational levels with $j \neq 0$ will not change significantly from the overlap integral for which $j = 0$.

The importance of this continuum emission process in accounting for features in low resolution or long exposure spectra is most evident where this emission peaks (~ 1575 Å). If the Lyman continuum were not included in the synthetic spectrum, shown as the bottom curve in Fig. 5, the mismatch around 1575Å (by about a factor of 2) with the measured spectrum is readily apparent.

VI. The H_2 Continuum

The so-called H_2 continuum is that rather featureless emission evident beyond 1650 in Fig. 1. This continuum emission spans the spectrum

from ~1400 Å to ~ 7000 Å, and is a result of radiative decay from the a $^3\Sigma_g^+$ levels to the b $^3\Sigma_u^+$ state, after dipole-forbidden excitation from the ground state.

The history of the study of the continuum emission is long and rich. In 1928 Winans and Stueckelberg[23] were the first to propose that the origin of the broad visible continuum evident in H_2 discharges was radiative decay from the a $^3\Sigma_g^+$ state to the newly discovered b $^3\Sigma_u^+$ repulsive state. (See Fig. 2.) As early as 1931, Finkelnberg and Weizel[24] attempted to quantify both the experiment (relative intensity vs. wavelength) and the theory. But the name which should be most associated with the problem is that of A. S. Coolidge. Beginning in 1936 he, James and Present[21] worked out what was essentially the correct theory for the emission process. (They derived Eq. 5.) Yet the calculated spectral shape did not agree with the experimental one. In 1938 James and Coolidge[25] again attacked the problem, this time using more accurate potential curves and calculating the matrix elements without using the Franck-Condon approximation. Still the comparison with experiment was unsatisfactory. Finally, in 1944 Coolidge[26] built an H_2 lamp and measured the spectrum himself to obtain convincing agreement with the theory.

A. Excitation to the a $^3\Sigma_g^+$ State

The population densities $n_{v'j'}$ of the a $^3\Sigma_g^+$ levels are also governed by Eq. 2. Yet in this case, the excitation rate coefficients are for transitions which are dipole forbidden, and the upper state lifetimes are determined by decay to the repulsive b $^3\Sigma_u^+$ state. Excitation from the singlet ground state to the triplet state is dipole forbidden because it involves a

change in the total electron spin angular momentum. This process does occur by electron excitation, but with a cross-section which falls off rapidly beyond threshold, since the excitation is accompanied by electron exchange. To the author's knowledge this cross-section has not yet been measured. Thus it is assumed to have a shape which decreases as $(E_{v''j''}^{v'j'}/E)^2$ beyond threshold, characteristic of the singlet-triplet excitation in He[27]. (E is the electron energy.) In a manner analogous to the $B\ ^1\Sigma_u^+$ excitation, the cross-section is assumed to be proportional to the overlap integrals between the ground and the $a\ ^3\Sigma_g^+$ vibrational wavefunctions[28]. It is further assumed that the rotational state is not altered in the excitation process. (It is changed by ±1 in a dipole transition. See Sect.III.)

From these relative cross-sections, relative excitation rate coefficients are calculated. Finally the constant of proportionality is adjusted until a satisfactory match with the measured spectrum (Fig. 1) is obtained. In other words, the measured spectrum and the absolute cross-sections for excitation to the $B\ ^1\Sigma_u^+$ levels are used to determine the absolute cross-section for excitation to the $a\ ^3\Sigma_g^+$ levels. The cross-section for excitation from the v" = 0 vibrational level of the $X\ ^1\Sigma_g^+$ state to all vibrational levels of the $a\ ^3\Sigma_g^+$ state is found to be:

$$\sum_{v'} \sigma_{v''=0}^{v'} = 1^{+2}_{-0.5} \times 10^{-18}\ (E_{th}/E)^2 \quad cm^2$$

for $E > E_{th} = 12.5$ eV, the weighted average-threshold-energy. (Note that, for the cases considered here, levels with v" > 0 are significantly populated. The cross-section is given in this way because Ajello et al.[4] expressed the excitation cross-section to the $B\ ^1\Sigma_u^+$ state in this way.)

B. Radiative Decay to the b $^3\Sigma_u^+$ State

The radiative decay to the continuum of levels in the repulsive b $^3\Sigma_u^+$ state is also described by Eq. 5, but with different initial and final states in the dipole matrix elements. It was recognized by Doyle[29] that the inclusion of rotational levels in the upper state with $j' > 0$, does not lead to a mild broadening of the spectral features (as it does for the Lyman continuum), since the argument given at the end of Section V no longer holds. In this case, since the two states have quite dissimilar potential curves, the addition of rotational energy significantly affects the overlap integrals. The state of rotation of both the initial and final state must be included explicitly in the calculation of the matrix elements required for the transition probabilities. These dipole matrix elements have been calculated by Doyle[29] for initial states with $v' = 0$ through 7, each with j' from 0 to approximately 20. For each initial state and for both R and P branch transitions, final states with energies corresponding to emission at 10 specified wavelengths from 1400 Å to 6667 Å were used. Interpolation was used to predict emission at other wavelengths.

The transition probabilities determined by Doyle were also used to calculate the lifetime for each v',j' level of the upper state required by Eq. 2 for knowledge of the upper level densities. This was accomplished by integrating the transition probabilities from a given v',j' level over all decay channels (R and P branch decays resulting in emission at any energetically-allowed wavelength).

VII. Discussion and Summary

The emissions from each of the three modeled processes (the Lyman

bands, the Lyman continuum, and the H_2 continuum) have been combined to produce synthetic spectra. The relative shapes of the synthetic spectra are functions of the three following variables:

T - the temperature of the H_2 ground state distribution,

T_e - the temperature of the exciting electrons, which enters through the excitation rate coefficients,

and the magnitude of the singlet-triplet excitation cross-section relative that for B $^1\Sigma_u^+$ excitation. The absolute volume emission rates are linearly dependent upon the unknowns, N_o and n_e, and are also dependent upon T_e. The comparison between the measured spectrum, shown in Fig. 1, and a synthetic spectrum, with T = 5000 °K, T_e = 1 eV, and the singlet-triplet excitation cross-section given in Sect. VI, is shown in Fig. 5. The agreement is quite good. The comparisons of the measured spectrum with synthetic spectra for which T = 4000 °K, T_e = 1 ev or T = 6000 °K, T_e = 3 eV are in obvious disagreement. This gives some indication about the sensitivity of the method as a diagnostic. Measured absolute emission rates, of course, yield the value of the product $N_o\ n_e$.

A more interesting emission source to which the models described here may be applied is the Alcator C Tokamak discharge. The H_2 emission comes from the 1-10 eV region at the plasma periphery. Since this is pulsed discharge, the spectrum in the 30 Å region around 1608 Å has been measured on a shot-by-shot basis over the course of ~ 40 reproducible discharges. This spectrum is shown in Fig. 6 with the stars and open circles. (The open circles indicate division of the measured intensity by 5, due to the presence of the OVII-1623Å line.) A predicted spectrum for T = 5000

°K and T_e = 3 eV is shown for comparison. Over this small region the shape of the predicted spectrum is not sensitive to the electron temperature, although it is sensitive to the H_2 temperature. For example, spectra with T = 3000 °K and T = 7000 °K are in much poorer agreement.

A detailed model for H_2 excitation by electrons in the 1 eV < T_e < 10 eV range has been described. The subsequent radiative decay, leading to the Lyman bands, the Lyman continuum, and the H_2 continuum, has also been described. The predictions of this model have been compared with measured spectra from three discharges. Quantitative agreement has been found in each case. This has been done as a first step in attempting to understand the role of the molecular hydrogen found in the edge plasma of high temperature, magnetically confined discharges.

Acknowledgements

This work was supported by U.S. Dept. of Energy Contract #DEAC02-78ET51013.

The author would like to acknowledge many useful discussions with Dr. Kate Kirby at the Harvard-Smithsonian Center for Astrophysics. In addition, he would like to thank the scientific and technical staff of the Alcator C Tokamak, Prof. A. Dalgarno for the use of the computer program used to calculate the Lyman continuum, Prof. H. W. Moos at Johns Hopkins for the use of the 1/8th m monochromator, G. H. Mount at the Univ. of Colorado, Boulder, for the high resolution H_2 spectrum in Fig. 3, and Y. L. Yung at Cal. Tech.

References

[1] Hinnov, E., et al., Princeton Univ. Plasma Physics Lab. Report MATT-270, (1964).

[2] McNeill, D. H., Bull. Am. Phys. Soc., 21 (1976), 1117.

[3] Terry, J. L., Bull. Am. Phys. Soc., 25 (1980), 951.

[4] Ajello, J. M., et al., Phys. Rev. A, 25 (1982), 2485-2498.

[5] Yung, Y. L., et al., Ap. J. (Letters), 254 (1982), L65-L69.

[6] Sharp, T. E., Atomic Data 2, (1971), 119-169.

[7] Fairfax, S. A., et al., in Plasma Physics and Controlled Nuclear Fusion Research (Proc. 8th Int. Conf. Brussels, 1980), Vol. 1, IAEA, Vienna (1981)

[8] Oren, L., Taylor, R. J., Nucl. Fusion, 17 (1977), 1143.

[9] Fastie, W. G., Kerr, D. E., Applied Optics, 14 (1975), 2133.

[10] Herzberg, G., Howe, L. L., Can. J Phys., 37 (1959), 639-659.

[11] Herzberg, G., Spectra of Diatomic Molecules, 2nd Ed. (D. Van Nostrand Co, Inc.), New York (1950).

[12] Lane, N. F., Rev. of Mod. Phys., 52 (1980), 29-119.

[13] Ehrhardt, H., et al., Phys. Rev., 173 (1968), 222-230.

[14] Turner, J., Kirby-Docken, K., Dalgarno, A., Ap. J. Suppl., 35 (1977), 282-292.

[15] Green, S., et al., Ap. J. Suppl., 36 (1978), 486-496.

[16] Elitzur, M., Watson, W. D., Astron. Astrophys., 70 (1978), 443-446.

[17] Green, S., Truhlar, D. G., Ap. J. (Letters), 231 (1970), L101-L103.

[18] Allison, A. C., Dalgarno, A., Atomic Data, 1 (1970), 289-304.

[19] Stephens, T. L.,Dalgarno, A., J. Quant. Spectrosc. Radiant. Transfer., 12 (1971), 569-586.

[20] Dalgarno, A., Herzberg, et al., Ap. J. (Letters), 162 (1970), L49-L53.

[21] Coolidge, A. S., et al., J. Chem. Phys., 4 (1936), 193-211.

[22] Stephens, T. L., PhD Thesis - Harvard University (1970) unpublished.

[23] Winans, J. G., Stueckelberg, E., Proc. Nat. Acad. Sci., 14 (1928), 867.

[24] Finkelnberg, W., Weizel, W., Zeits. f. Physik, 68 (1931), 577.

[25] James, H. M., Coolidge, A. S., Phys. Rev., 55 (1939), 184-190.

[26] Coolidge, A. S., Phys. Rev., 65 (1944), 236-246.

[27] Moiseiwitsch, B. L., Smith, S. J., Rev. of Mod. Phys. 40 (1968), 238.

[28] The a complete set of overlap integrals between the X $^1\Sigma_g^+$ vibrational wavefunctions and those of the a $^3\Sigma_g^+$ state was not available. It was assumed that they are proportional to those between the ground and the C $^1\Pi_u$ state, which lies close to the a $^3\Sigma_g^+$ state. Calculation of the correct overlap integrals is in progress.

[29] Doyle, R. O., PhD Thesis - Harvard University (1965), unpublished.

Figure Captions

Figure 1. The Far UV spectum of H_2, emitted from the 'discharge cleaning' plasma in Alcator C. The instrumental resolution was 3 Å; the instrumental sensitivity has been compensated.

Figure 2. The potential curves for the X $^1\Sigma_g^+$ electronic ground state, the B $^1\Sigma_u^+$ state, the a $^3\Sigma_g^+$ state, and the repulsive b $^3\Sigma_u^+$ state (from [5]).

Figure 3. (top trace) A high resolution spectrum showing the bound-bound Lyman transitions around 1600 Å. (bottom trace) The same region of the spectrum synthesized by the model described in the text for T = 450 °K.

Figure 4. Schematic representation of excitation from v" = 0 of the ground electronic state to v" = 9 of the $B^1\Sigma_u^+$ state, followed by decay back to the vibrational continuum. This results in Lyman continuum emission. Vibrational wavefunctions are shown.

Figure 5. A detailed comparison between the measured spectrum from the Alcator C 'discharge cleaning' plasma (top trace) and a synthetic spectrum with T = 5000 °K and T_e = 1 eV (bottom trace). The zero of the measured spectrum is displaced by a constant amount for comparison.

Figure 6. The data points are the spectrum measured from a high temperature discharge in the Alcator C Tokamak. (Note that the values for the open circles have been divided by 5 and are due to OVII-1623 Å line emission.) The solid curve is the predicted spectrum for T = 5000 °K and T_e = 3 eV.

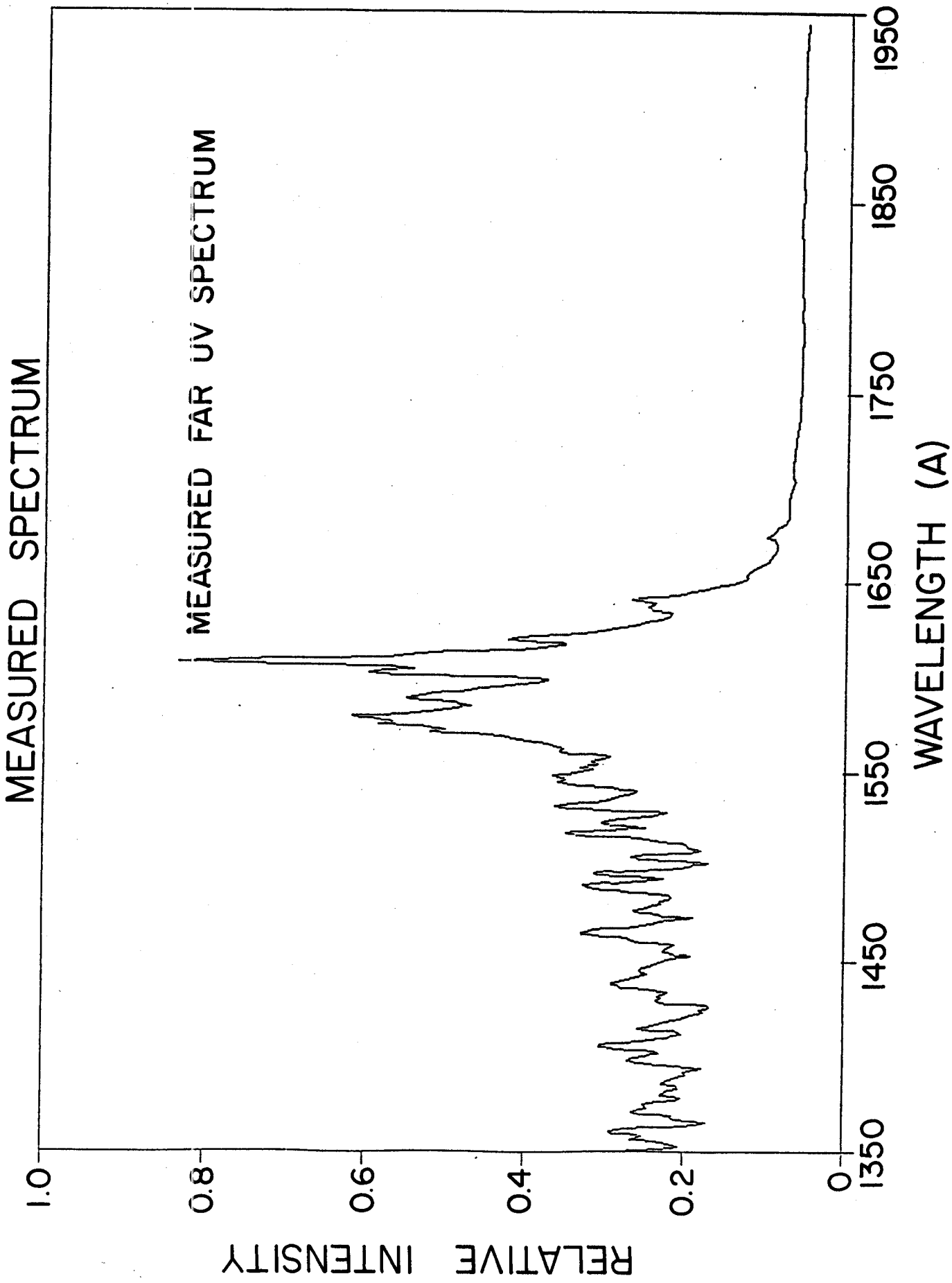
MEASURED SPECTRUM
MEASURED FAR UV SPECTRUM
RELATIVE INTENSITY
1.0
0.8
0.6
0.4
0.2
0
1350
1450
1550
1650
1750
1850
1950
WAVELENGTH (A)

FIGURE 1.

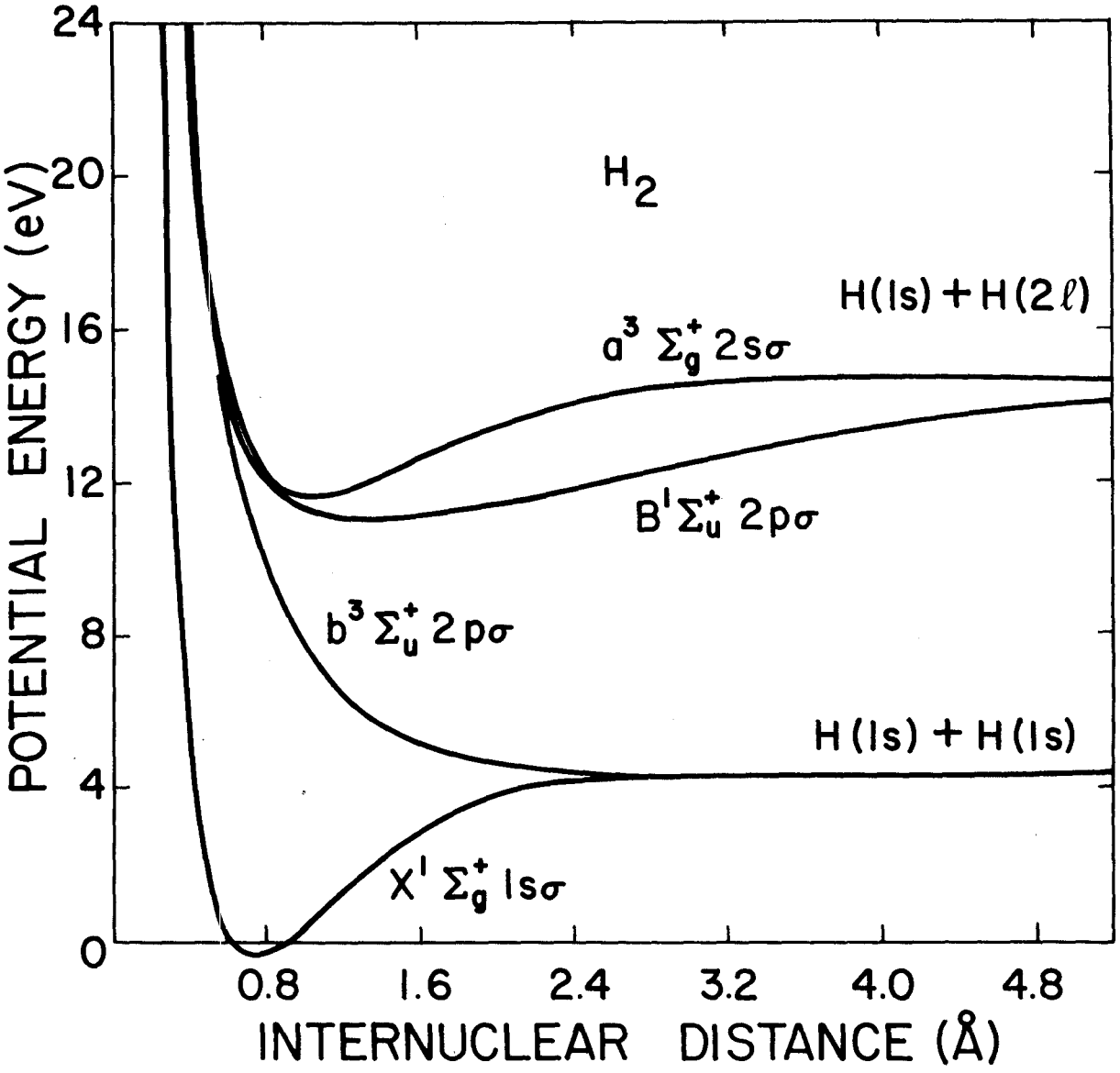

PFC-8041

FIGURE 2.

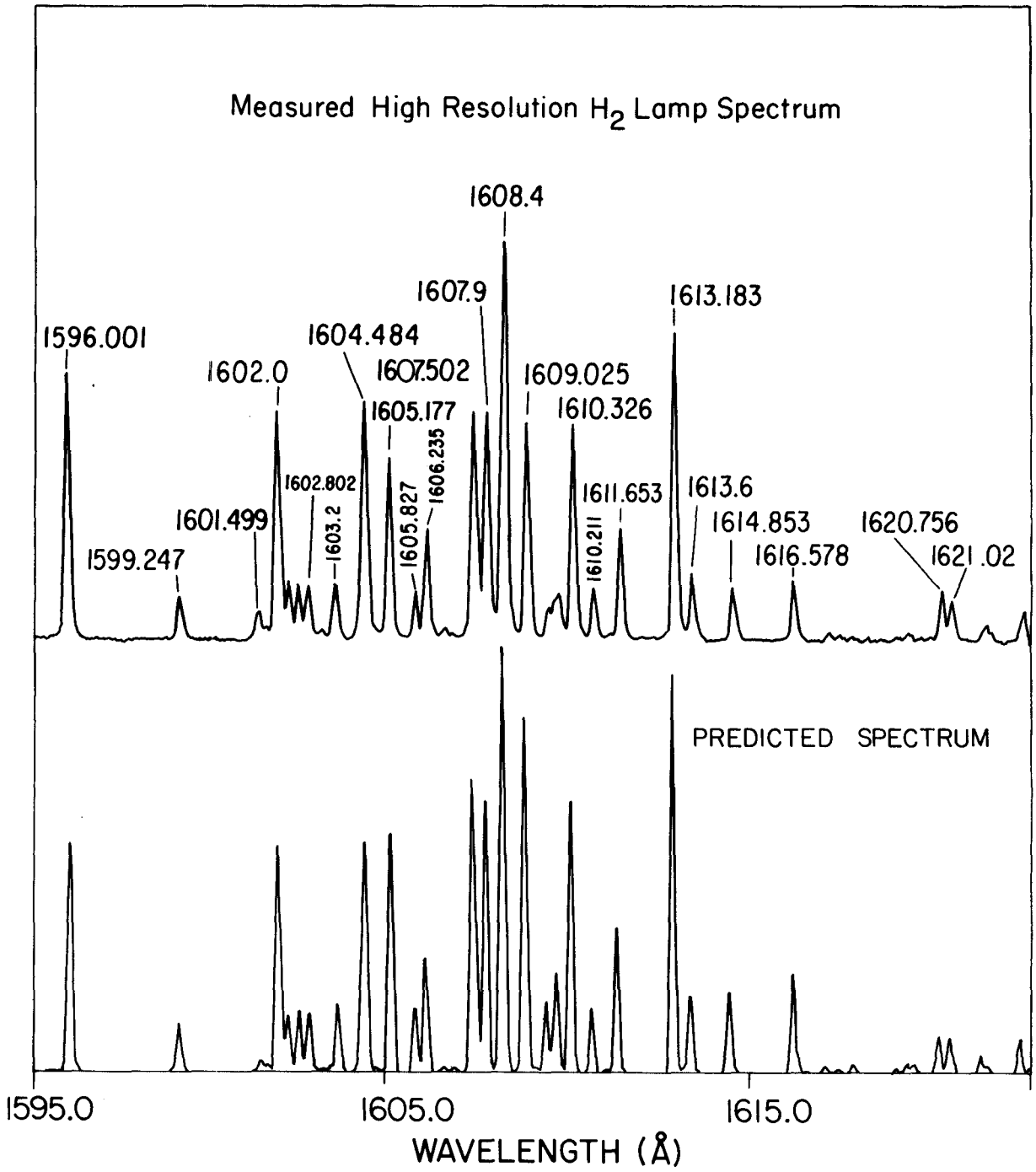
Measured High Resolution H_2 Lamp Spectrum
1608.4
1607.9
1613.183
1596.001
1604.484
1602.0
1607.502
1609.025
1610.326
1605.177
1606.235
1602.802
1611.653
1613.6
1601.499
1603.2
1605.827
1610.211
1614.853
1620.756
1599.247
1616.578
1621.02
PREDICTED SPECTRUM
1595.0
1605.0
1615.0
WAVELENGTH (Å)

FIGURE 3.

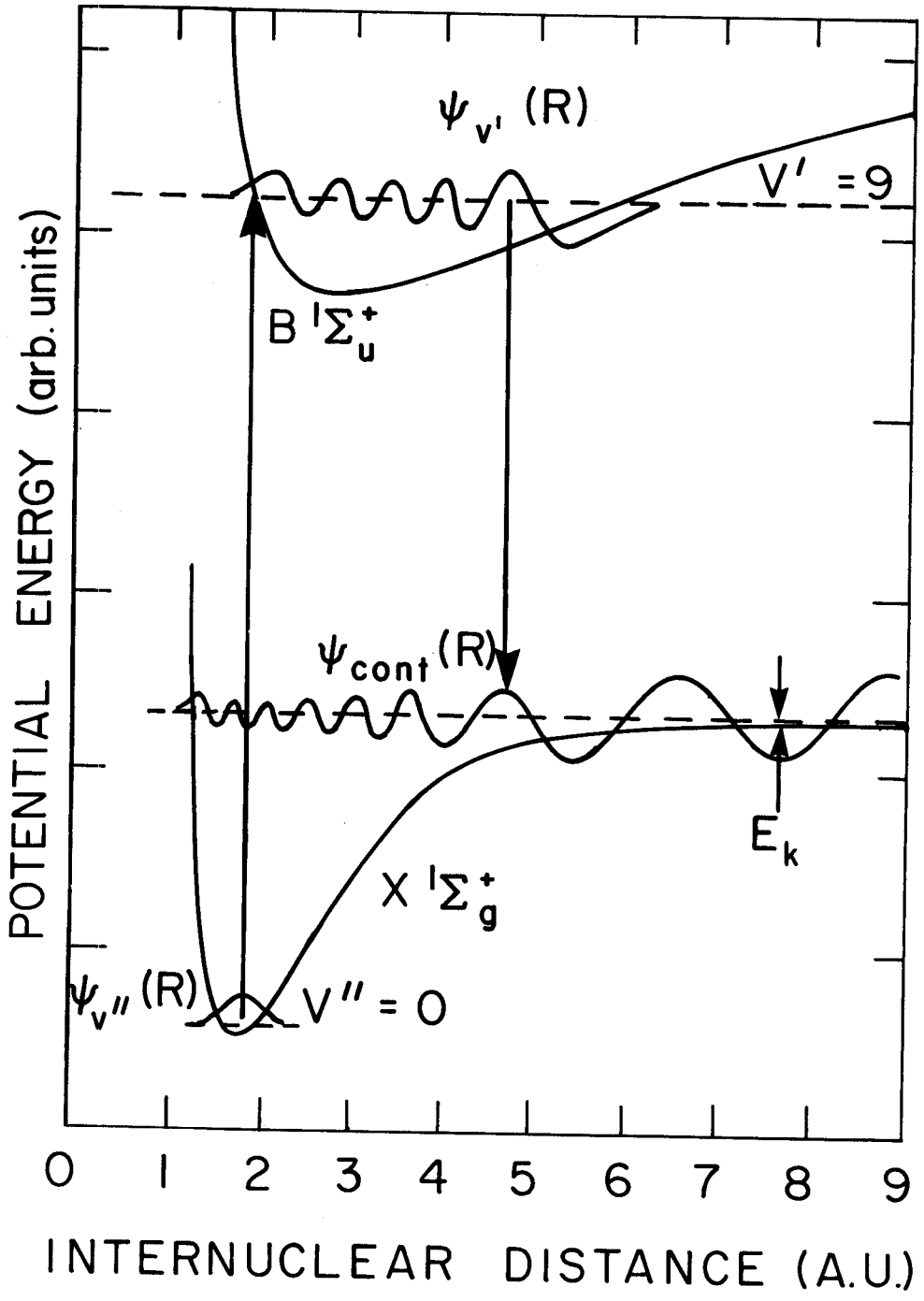
$\psi_{v'}$ (R)
V′ =9
B $^1\Sigma_u^+$
ψ_{cont} (R)
E_k
X $^1\Sigma_g^+$
$\psi_{v''}$ (R)
V″ = 0
POTENTIAL ENERGY (arb.units)
0 1 2 3 4 5 6 7 8 9
INTERNUCLEAR DISTANCE (A.U.)

FIGURE 4.

FIGURE 5.

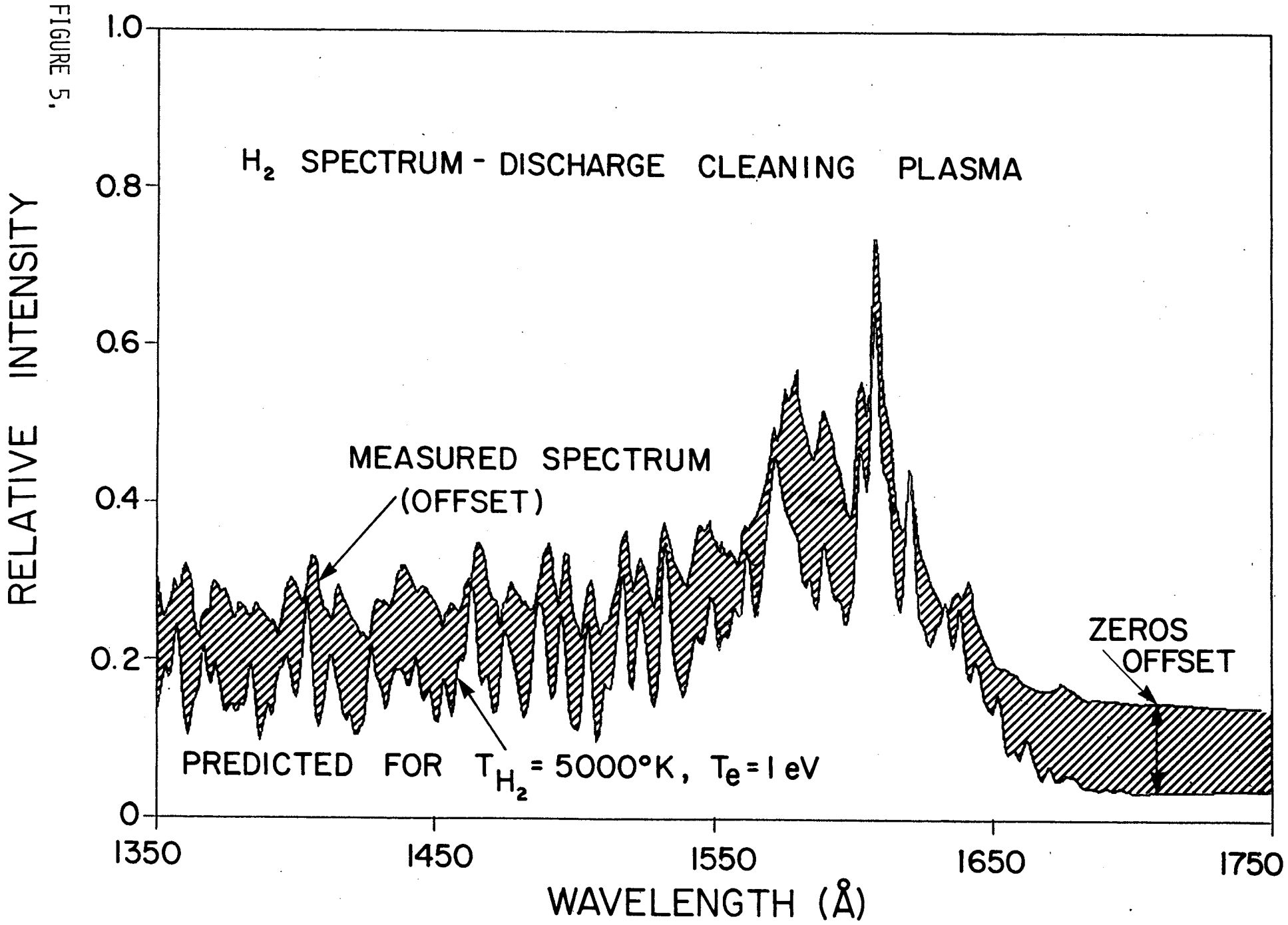
H_2 SPECTRUM - DISCHARGE CLEANING PLASMA
MEASURED SPECTRUM
(OFFSET)
ZEROS
OFFSET
PREDICTED FOR T_{H_2} = 5000°K, T_e = 1 eV
RELATIVE INTENSITY
1.0
0.8
0.6
0.4
0.2
0
1350
1450
1550
1650
1750
WAVELENGTH (Å)

FIGURE 6.

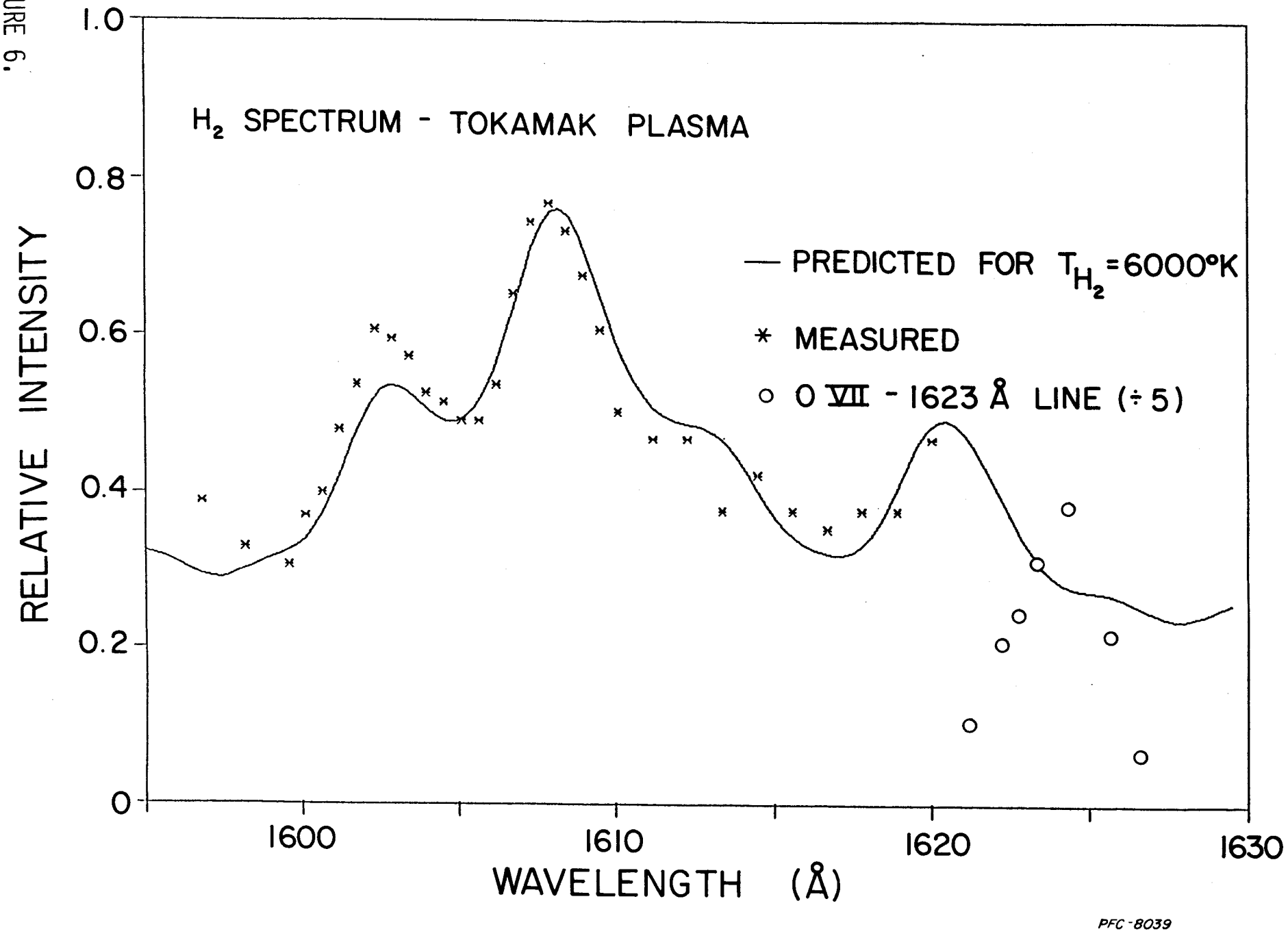
H_2 SPECTRUM - TOKAMAK PLASMA
— PREDICTED FOR T_{H_2} = 6000°K
* MEASURED
○ O VII - 1623 Å LINE (÷ 5)
RELATIVE INTENSITY
1.0
0.8
0.6
0.4
0.2
0
1600
1610
1620
1630
WAVELENGTH (Å)
PFC-8039